Superconductivity appears in the vicinity of semiconducting-like behavior in $CeO_{1-x}F_xBiS_2$

Jie Xing, Sheng Li, Xiaxin Ding, Huan Yang, and Hai-Hu Wen*

National Laboratory of Solid State Microstructures and Department of Physics, Center for Superconducting Physics and Materials, Nanjing University, Nanjing 210093, China

(Received 24 August 2012; published 28 December 2012)

Resistive and magnetic properties have been measured in BiS_2-based samples $CeO_{1-x}F_xBiS_2$ with a systematic substitution of O with F ($0 < x < 0.6$). In contrast to the band-structure calculations, it is found that the parent phase of $CeOBiS_2$ is a bad metal instead of a band insulator. By doping electrons into the system, it is surprising to find that superconductivity appears together with a semiconducting normal state. This evolution is clearly different from the cuprate and the iron pnictide systems, and is interpreted as approaching the Pomeranchuk transition with a von Hove singularity and the possible charge-density-wave instability. Furthermore, ferromagnetism, which may arise from the Ce magnetic moments, has been observed in the low-temperature region in all samples, suggesting the coexistence of superconductivity and ferromagnetism in the superconducting samples.

DOI: 10.1103/PhysRevB.86.214518 PACS number(s): 74.70.Dd, 74.20.Mn, 74.25.Dw, 74.25.fc

I. INTRODUCTION

In the past decades, several new superconducting systems with layered structures have been discovered.[1–4] Empirically, it is even anticipated that exotic superconductivity may be achieved with the layered, tetragonal, or orthorhombic structures of compounds containing $3d$ or $4d$ transition metals, because the correlation effect is somehow strong in these types of samples. In this context, cuprates and iron pnictides/chalcogenides are typical examples. In both systems, the parent phase is either a Mott insulator, as in the cuprates, or a bad metal, as in the iron pnictides/chalcogenides. Through doping charges, the electric conduction of the samples becomes much improved and superconductivity sets in gradually. At the optimal doping point where the superconducting transition temperature is the highest, the resistivity is exhibited normally as a metallic behavior, and sometimes a linear temperature dependence of resistivity shows up as evidence of quantum criticality. Quite recently, Mizuguchi *et al.* discovered the novel BiS_2-based superconductor $Bi_4O_4S_3$ (called the 443 system) with $T_c^{\rm onset} = 8.6$ K.[5] This material has a BiS_2 layer with $I4/mmm$ structure. Several days later, another BiS_2-based superconductor, namely $LaO_{1-x}F_xBiS_2$ (called the 1112 system), was reported.[6] Using transport and magnetic measurements, we concluded that multiband and exotic superconductivity exist in $Bi_4O_4S_3$.[7] This is interesting and unexpected, and people are curious to know what induces the exotic superconductivity here. Using the high-pressure synthesizing method, it was found that T_c can reach 10.6 K in $LaO_{1-x}F_xBiS_2$.[6] In the meantime, other groups repeated the discovery of superconductivity in BiS_2-based systems.[7–9] By replacing La with Nd, superconductivity was also discovered at about $T_c^{\rm onset} = 5.6$ K.[10] Scrutiny of the structures of all these samples finds that the BiS_2 layers may be the common superconducting planes in the compounds with many different blocking layers. The first-principles band-structure calculation indicated that the superconductivity was derived from the Bi $6p_x$ and $6p_y$ orbitals and might be related to the strong nesting effect of the Fermi surface and quasi-one-dimensional bands.[11] A pressure experiment has been done on $Bi_4O_4S_3$ and $LaO_{1-x}F_xBiS_2$ (Ref. 12) samples, and the results indicate that the Fermi surface is located in the vicinity of some band edges leading to instability for superconductivity in $LaO_{1-x}F_xBiS_2$. Because of this, it would be interesting to substitute La with another element such as Ce in BiS_2-based 1112 materials since it can change the chemical pressure. Additional results from band-structure calculation also indicate a strong Fermi surface nesting effect.[13] Possible pairing symmetries were also discussed based on the random-phase approximation (RPA).[11,14] In this paper, we report on the superconductor $CeO_{1-x}F_xBiS_2$ with a typical BiS_2 layer and a $P4/nmmz$ space group. It is found that the parent phase is a bad metal instead of a band insulator. Meanwhile, the superconductivity appears along with a normal state with semiconducting behavior, showing sharp contrast with the cuprates and the iron pnictides.

II. SAMPLE PREPARATION AND THE EXPERIMENTAL METHODS

The polycrystalline samples were grown by a conventional solid-state reaction method. First of all, we mixed Ce flakes (99.9%, Alfa Aesar), CeF_3 (99.9%, Alfa Aesar), CeO_2 (99.9%, Alfa Aesar), Bi_2S_3 (99.9%, Alfa Aesar), and S powder (99.9%, Alfa Aesar) using the ratio in the stoichiometry $CeO_{1-x}F_xBiS_2$. Secondly, we pressed the mixture into a pellet shape and sealed it in an evacuated quartz tube. Then it was heated up to 700 °C and kept for 10 h. After cooling the compound to room temperature slowly, the product was well mixed by regrinding, pressed into a pellet shape, and annealed at 600 °C for 10 h. The obtained samples looked black and hard. The true composition of the samples was checked with energy-dispersive x-ray spectroscopy (EDX) analysis on randomly selected grains and found to be close to the nominal one. The crystallinity of the sample was measured by x-ray diffraction (XRD) using a Brook Advanced D8 diffractometer with Cu $K\alpha$ radiation. The analysis of the XRD data was performed with the software POWDER-X and TOPAS. From the PDF-2 2004, we can see that the XRD pattern looks very similar to the result of standard samples of $CeOBiS_2$. The Rietveld fitting shows that over 90% of the samples are $CeO_{1-x}F_xBiS_2$ and fewer than 10% are derived from the impurities, which is mainly Ce_2O_2S. As

the sample is hard enough, we can cut and polish it into a barlike shape with a lateral surface of rectangular shape for sequential transport measurements. The resistivity and Hall effect were measured with Quantum Design instrument PPMS-9T. The magnetization was detected by the Quantum Design instrument SQUID-VSM with a resolution of about 5×10^{-8} emu. The six-lead method was applied for the transport measurement on the resistivity and Hall effect simultaneously. The Hall effect was measured by either sweeping the magnetic field at a fixed temperature or sweeping the temperature at a fixed magnetic field. The data obtained by these two methods coincide with each other.

III. RESULTS AND DISCUSSION

Figure 1 shows the x-ray diffraction data for the powdered samples of $CeO_{1-x}F_xBiS_2$ ($x = 0$–0.6). The space group of the standard $CeOBiS_2$ is $P4/nmmz$ with a layered structure. The XRD pattern looks very similar to the standard $CeOBiS_2$ with a few minor peaks of the impurity phase. The Rietveld fitting result also reveals that the a axis of $CeO_{1-x}F_xBiS_2$ is 4.016 Å at $x = 0$, increases to 4.038 Å until $x = 0.5$, and then decreases to 4.037 Å at $x = 0.6$. The c-axis lattice constant decreases from 13.607 to 13.343 Å continuously as x is increased from $x = 0$ to 0.6. This result indicates that the layer structure expands in the in-plane direction as more F elements are doped into the system, reaches a maximum at $x = 0.5$, and then starts to shrink at $x = 0.6$. The smooth decrease of the c-axis lattice

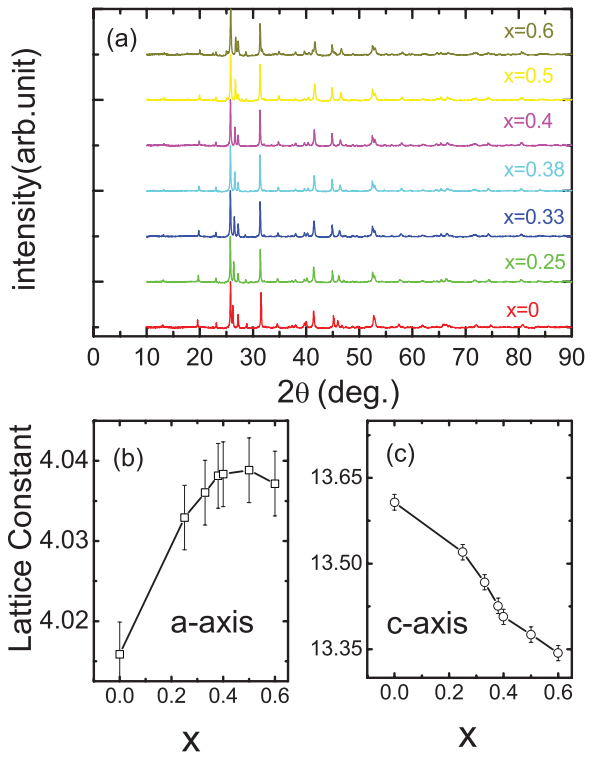

FIG. 1. (Color online) The x-ray diffraction profile for the powdered samples of $CeO_{1-x}F_xBiS_2$ ($x = 0$–0.6). Except for several minor peaks of impurities, all of the peaks can be characterized to the standard $CeOBiS_2$ with the space group $P4/nmmz$. Parts (b) and (c) show the doping dependence of the lattice constants of the a axis and the c axis, respectively.

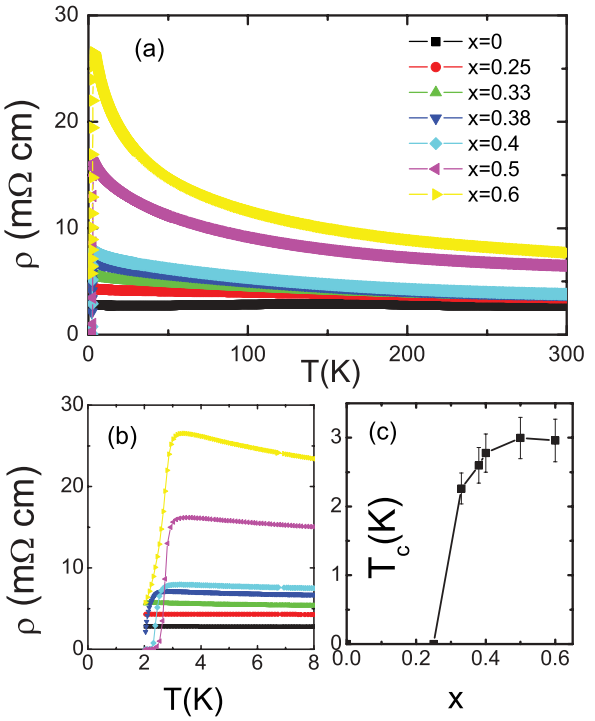

FIG. 2. (Color online) (a) The temperature dependence of resistivity for $CeO_{1-x}F_xBiS_2$ ($x = 0$–0.6). It is clear that the parent phase at $x = 0.0$ is a bad metal, not a band insulator as expected by the LDA calculation. (b) An enlarged view of the same data in the low-temperature region. (c) The doping dependence of the superconducting transition temperature determined through the crossing method (see text).

parameter suggests that F has been successfully substituted to the O site, as the ionic radius of F is smaller than that of O. The results seem to be similar to that of $NdO_{1-x}F_xBiS_2$.[10]

In Fig. 2(a), we present the temperature dependence of resistivity for a different doped sample of $CeO_{1-x}F_xBiS_2$ with $x = 0$–0.6. It is clear that the parent phase $CeOBiS_2$ is not an insulator nor is it a superconductor. The temperature dependence of resistivity of the parent phase presents a nonmonotonic change from 2 to 300 K. Based upon the LDA calculation,[11] the parent phase of this kind of material should be a band insulator, as it is distinct from the experiment result. This could be due to two reasons: (i) There is a self-doping in the parent phase, so that it exhibits a metallic behavior instead of a band insulator. This is, however, not supported by the Hall effect measurement shown below. The Hall data indicate that the parent phase is dominated by the electron-charge carriers. By further doping F to O sites, one induces more electrons into the system, therefore a better metallic behavior should be anticipated. But actually the system becomes more insulating-like with further doping. (ii) The metallic behavior of the parent phase may be induced by the strong spin-orbital coupling, which shifts the bottom of the p_x and p_y bands below the Fermi energy. The same data with an enlarged scale are shown in Fig. 2(b). It is easy to see that superconductivity appears at about $x = 0.33$ and the transition become sharpest at $x = 0.5$ with the highest transition temperature. The onset of the superconducting transition in the sample with $x = 0.5$ is about 3.0 K as determined by the so-called crossing method,

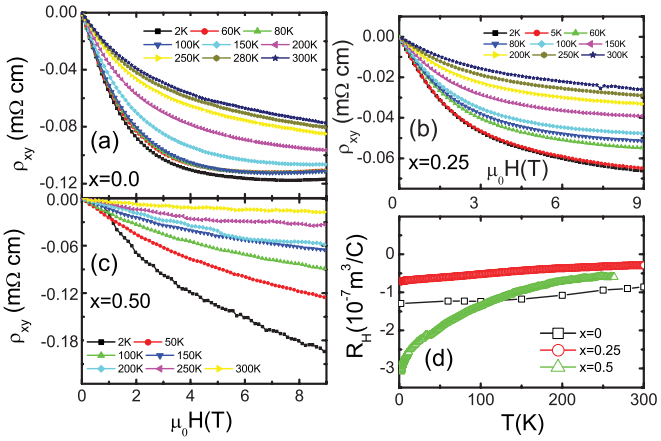

FIG. 3. (Color online) (a) The Hall resistivity ρ_{xy} vs the magnetic field $\mu_0 H$ at 2, 60, 80, 100, 150, 200, 250, 280, and 300 K for the sample $CeO_{1-x}F_xBiS_2$, $x = 0$. (b) The Hall resistivity ρ_{xy} vs the magnetic field $\mu_0 H$ at 2, 5, 60, 80, 100, 150, 200, 250, 280, and 300 K for sample $CeO_{1-x}F_xBiS_2$, $x = 0.25$. (c) The Hall resistivity ρ_{xy} vs the magnetic field $\mu_0 H$ at 2, 50, 100, 150, 200, 250, and 300 K for sample $CeO_{1-x}F_xBiS_2$, $x = 0.5$. (d) The Hall coefficient R_H of the three samples ($CeO_{1-x}F_xBiS_2$, $x = 0.0, 0.25$, and 0.5) at 9 T from 2 to 300 K. The dense data points for $x = 0.25$ and 0.50 were determined by the measurements at -9 and 9 T by sweeping temperature. The discrete data points for $x = 0$ were determined from the measurements by sweeping the magnetic field at a fixed temperature.

that is, the crossing point between a normal state straight line and an extrapolation line of the steep transition part. From Fig. 2(b), we can also realize that the resistivity of these materials increases with the doping of the F concentrations. It is very strange to see that superconductivity and an insulating-like or semiconducting normal state appear together. In Fig. 2(c), the doping dependence of the superconducting transition temperature is shown. It is clear that a half-dome-like superconducting area is observed here. Actually, in most 1112 samples reported so far, the superconductivity emerges in the background of insulating-like or semiconducting behavior.[6,12]

To reveal the strange normal state behavior, we measured the Hall effect of three samples with $x = 0.0$, 0.25, and 0.5. Figures 3(a)–3(c) show the magnetic field dependence of the Hall resistivity ρ_{xy} at different temperatures of the three samples. Here ρ_{xy} was measured with a longitudinal current with the magnetic field perpendicular to the current and the surface of the platelike sample, and the voltage V_{xy} was taken at the direction across the sample width. Figure 3(d) shows the temperature dependence of R_H of the three samples determined at a magnetic field of 9 T. Normally for a single-band metal or a semiconductor, the Hall coefficient R_H can be measured by $R_H = d\rho_{xy}/dH = 1/ne$, with n the charge carrier density when ρ_{xy} exhibits a linear behavior with the magnetic field. However, as we saw in the previous study in the system of $Bi_4S_4O_3$, the Hall resistivity is extremely nonlinear in a magnetic field, making it difficult to determine R_H in the usual way. For a multiband system, to unravel the different scattering rates from the different individual bands, a high magnetic field is required, otherwise only the scattering message from partial bands is detected. This is why we choose to use the 9 T data. We thus determine R_H here directly by $R_H = \rho_{xy}/H$ at 9 T. All of these results show that the ρ_{xy} of the three samples is negative from 2 to 300 K at 9 T, indicating that the electronlike charge carriers are the dominating one. From Figs. 3(a) and 3(b), one can see that the magnetic field dependence of ρ_{xy} is more curved at low doping levels. This illustrates that there may be a very strong multiband effect or a shallow band-edge effect at these phases. With more doping, the nonlinear curvature seems weakened slightly. In Fig. 3(d), one can clearly see that the Hall coefficient R_H of the low doped samples ($x = 0.0$ and 0.25) has a weak temperature dependence. Qualitatively, it is further suggested that more electrons are doped to the system since the charge-carrier density determined from $n = 1/R_H e$ is higher in the sample of $x = 0.25$ than that of $x = 0.0$. This may suggest that these samples are more or less dominated by a single band at low doping while having a shallow band edge for both the p_x and p_y bands, so that ρ_{xy} exhibits a nonlinear field dependence. We can use the single-band assumption to estimate the charge-carrier density, which is about $10^{19}/cm^3$, supporting the idea of a shallow band edge or a small Fermi pocket. As for the sample with $x = 0.5$, the Hall coefficient shows a very strong temperature dependence, indicating that multiscattering channels are involved. Interestingly, the superconductivity occurs at the same time. This suggests that the later joined scattering is very important for superconductivity. One picture derived from the data would be that the system is closer to the Van Hove singularity point as the doping gets closer to 0.5. The LDA calculation[11] does indicate that the Fermi surface segments will emerge at the middle point between the Γ (A) and M (Z) points, leading to a high density-of-states (DOS) peak (the von Hove singularity effect). At the doping level of $x = 0.5$, the Fermi surface also has a Pomeranchuk transition from four small Fermi pockets at ($\pm\pi$,0) and (0,$\pm\pi$) to a complete larger one. The huge DOS peak near the Fermi energy due to the von Hove singularity provides a pairing instability. Meanwhile, the large Fermi surface has a parallel part near ($\pm\pi/2$, $\pm\pi/2$). It may be this better-achieved nesting effect of the Fermi surface in the higher doped samples that leads to a charge-density-wave (CDW) instability, which results in the enhanced semiconducting background. In the meantime, as is often the case in a multiband system, some of the electrons pair and condense in order to lower the system energy. The pressure study for BiS_2 superconductors also elucidates that the sample with $x = 0.5$ is located in the vicinity of some instability between the semiconducting and the metallic behavior.[12]

Figure 4 shows the magnetoresistance for the three typical samples of $x = 0.0$, 0.25, and 0.5. From Figs. 4(a)–4(c), it is easy to see that by increasing the electron doping, the magnetoresistance ρ_{xx} shows an enhanced linear character from $x = 0$ to 0.5. For the undoped sample, ρ_{xx} increases 20%–30% at a magnetic field of 9 T. This is in contrast to the sample with $x = 0.5$, where ρ_{xx} has only a 5% increase at 9 T. As the magnetoresistance of either a single-band or a two-band system should be proportional to H^2 in the low-field region, the rough linear field dependence of the magnetoresistance of the superconducting sample ($x \geqslant 0.25$) $CeO_{1-x}F_xBiS_2$ is really unique and strange. The result is similar to that seen in measurements on $Bi_4O_4S_3$.[7] A similar result was also seen

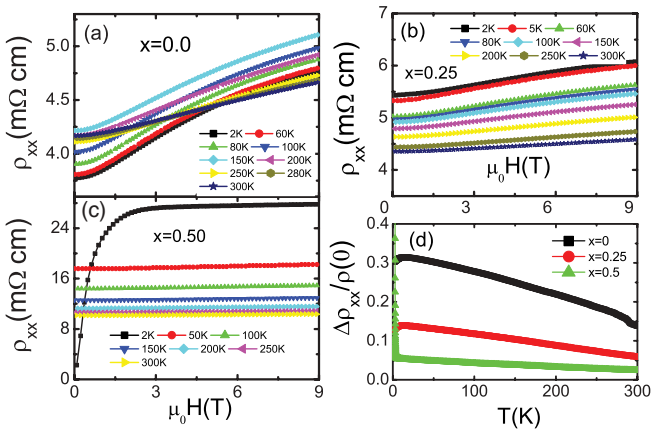

FIG. 4. (Color online) (a) Magnetic-field-dependent magnetoresistance ρ_{xx} at 2, 60, 80, 100, 150, 200, 250, 280, and 300 K for sample $CeO_{1-x}F_xBiS_2$ with $x = 0.0$. (b) Field dependence of magnetoresistance ρ_{xx} at 2, 5, 60, 80, 100, 150, 200, 250, and 300 K for sample $CeO_{1-x}F_xBiS_2$ with $x = 0.25$. (c) Field dependence of magnetoresistance ρ_{xx} at 2, 50, 100, 150, 200, 250, and 300 K for sample $CeO_{1-x}F_xBiS_2$ with $x = 0.5$. (d) Temperature dependence of the magnetoresistance $\Delta\rho_{xx}/\rho_0$ at 9 T for three samples of $CeO_{1-x}F_xBiS_2$ with $x = 0.0$, 0.25, and 0.5.

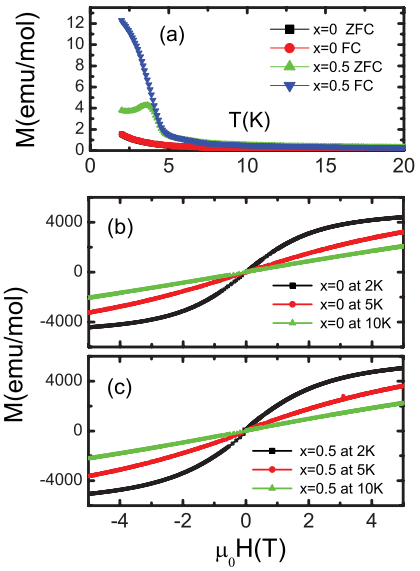

FIG. 5. (Color online) (a) Temperature dependence of the dc magnetization of the two samples $CeO_{1-x}F_xBiS_2$ with $x = 0.0$ and 0.5. (b) Isothermal MHLs at 2, 5, and 10 K of the sample $CeO_{1-x}F_xBiS_2$ with $x = 0.0$, showing a ferromagnetic transition below about 6 K. (c) The MHLs measured at 2, 5, and 10 K for the sample $x = 0.5$.

in $NbSe_2$,[15] which exhibits both superconductivity and the CDW effect. The anomalous linear field dependence of the magnetoresistance may be induced by the semiconducting effect in the normal state, probably due to the gradually enhanced CDW tendency. Figure 4(d) shows the temperature dependence of magnetoresistance of these three samples at 9 T. The trend shows that with electron doping, the magnetoresistance gets weaker, manifesting a stronger multiband effect in the underdoped samples. With more doping, the Fermi segments near $(\pm\pi/2,\pm\pi/2)$ will appear. This effect, on the one hand, will lead to the Van Hove singularity peak on the DOS at the Fermi energy, while on the other hand one complete large Fermi surface will be formed, which suppresses the multiband effect. Therefore, it is very important to approach the Von Hove singularity point and the Pomeranchuk transition of the Fermi surface versus doping for both superconductivity and the semiconducting behavior in the normal state.

In the superconducting samples, we did not succeed in obtaining the diamagnetic signal. At first glance, this seems to be in contradiction with the conclusion of a bulk superconductor, while a closer inspection finds that the superconducting diamagnetism is actually prevailed over by a quite strong ferromagnetism. In Fig. 5(a), we present the temperature dependence of magnetic susceptibility for $CeO_{1-x}F_xBiS_2$ ($x = 0.0$ and 0.5) at the field of 10 Oe. It is interesting to realize that the parent phase has already a ferromagnetic transition at approximately 5 K. The isothermal magnetization-hysteresis loops (MHLs) in Fig. 5(b) support this conclusion as well. As for the sample of $x = 0.5$, we see two steps on the zero-field-cooled magnetization curve, one occurring at about 5 K with an uprising of the magnetization, and the other with the relative dropping of the magnetization at about 3.7 K. From the resistive data, we see that the onset superconducting transition point is located at about 3 K as defined by the crossing point of the flat normal state background and the steepest resistive transition part. Therefore, the tiny magnetization step at around 3.7 K may not be associated with the superconducting transition. The observation of the diamagnetic transition may be hindered by the large ferromagnetic signal. The MHLs of the $x = 0.5$ sample shown in Fig. 5(c) indicate also the dominating ferromagnetic signal. This ferromagnetism may be induced by the local moment of Ce, or some exotic reasons related to the superconducting mechanism. For the superconducting sample, this indicates the coexistence of superconductivity and ferromagnetism at a low temperature. It remains to be discovered how the superconductivity occurring in the BiS_2 layers accommodates well the ferromagnetic order in the CeO layer, since bulk superconductivity requires establishing interlayer coupling across the ferromagnetic CeO layers. For a singlet pairing, this seems to be challenging.

IV. CONCLUDING REMARKS

In summary, we have fabricated a BiS_2-based superconducting system $CeO_{1-x}F_xBiS_2$ with a systematic substitution of O with F ($0.0 < x < 0.6$). Resistivity, the Hall effect, magnetoresistance, and magnetization have been measured. The parent phase is found to be a bad metal, which is not consistent with the LDA calculations. By substituting O with more F, superconductivity gradually appears along with a semiconducting-like normal state. By analyzing the Hall effect and the magnetoresistance and combining with the LDA calculations, we intend to conclude that the undoped or low-doped samples have a very shallow band edge with small Fermi pockets. However, when it is close to a doping level of $x = 0.5$, the system approaches a Von Hove singularity with the feature that the Fermi surface segments near $(\pm\pi/2,\pm\pi/2)$ will emerge leading to a Pomeranchuk transition. The semiconducting

behavior in the normal state of the superconducting sample is interpreted as either a charge-density-wave instability or a gradually enhanced correlation effect. Finally, we show the coexistence of the superconductivity with the ferromagnetic order state arising from the local moments of Ce at low temperatures.

ACKNOWLEDGMENTS

We appreciate the useful discussions with Liang Fu at Harvard and Fa Wang at MIT. This work is supported by the NSF of China, the Ministry of Science and Technology of China (973 projects: No. 2011CBA00102, No. 2010CB923002, and No. 2012CB821403), and PAPD.

*hhwen@nju.edu.cn

[1] J. G. Bednorz and K. A. Muller, Z. Phys. B **64**, 189 (1986).
[2] A. Ardavan, S. Brown, S. Kagoshima, K. Kanoda, K. Kuroki, H. Mori, M. Ogata, S. Uji, and J. Wosnitza, J. Phys. Soc. Jpn. **81**, 011004 (2012).
[3] J. Nagamatsu, N. Nakagawa, T. Muranaka, Y. Zenitani, and J. Akimitsu, Nature (London) **410**, 63 (2001).
[4] Y. Kamihara, T. Watanabe, M. Hirano, and H. Hosono, J. Am. Chem. Soc. **130**, 3296 (2008).
[5] Y. Mizuguchi, H. Fujihisa, Y. Gotoh, K. Suzuki, H. Usui, K. Kuroki, S. Demura, Y. Takano, H. Izawa, and O. Miura, arXiv:1207.3145.
[6] Y. Mizuguchi, S. Demura, K. Deguchi, Y. Takano, H. Fujihisa, Y. Gotoh, H. Izawa, and O. Miura, J. Phys. Soc. Jpn. **81**, 114725 (2012).
[7] S. Li, H. Yang, J. Tao, X. Ding, and H. H. Wen, arXiv:1207.4955.
[8] S. G. Tan, P. Tong, Y. Liu, W. J. Lu, L. J. Li, B. C. Zhao, and Y. P. Sun, Physica C **483**, 94 (2012).
[9] S. K. Singh, A. Kumar, B. Gahtori, S. Kirtan, G. Sharma, S. Patnaik, and V. P. S. Awana, J. Am. Chem. Soc. **134**, 16504 (2012).
[10] S. Demura, Y. Mizuguchi, K. Deguchi, H. Okazaki, H. Hara, T. Watanabe, S. J. Denholme, M. Fujioka, T. Ozaki, H. Fujihisa, Y. Gotoh, O. Miura, T. Yamaguchi, H. Takeya, and Y. Takano, arXiv:1207.5248.
[11] H. Usui, K. Suzuki, and K. Kuroki, Phys. Rev. B **86**, 220501 (2012).
[12] H. Kotegawa, Y. Tomita, H. Tou, H. Izawa, Y. Mizuguchi, O. Miura, S. Demura, K. Deguchi, and Y. Takano, J. Phys. Soc. Jpn. **81**, 103702 (2012).
[13] X. G. Wan, H. C. Ding, S. Y. Savrasov, and C. G. Duan, arXiv:1208.1807.
[14] T. Zhou and Z. D. Wang, arXiv:1208.1101.
[15] R. Corcoran, P. Meeson, Y. Onuki, P. A. Probst, M. Springford, K. Takita, H. Harima, G. Y. Guo, and B. L. Gyorffy, J. Phys.: Condens. Matter **6**, 4479 (1994).